Article

Photosensitized membrane permeabilization requires contact-dependent reactions between photosensitizer and lipids

Isabel Bacellar, Maria Cecília Oliveira, Lucas Dantas, Elierge Costa, Helena Couto Junqueira, Waleska Kerllen Martins, Andrés M. Durantini, Gonzalo Cosa, Paolo Di Mascio, Mark Wainwright, Ronei Miotto, Rodrigo Maghdissian Cordeiro, Sayuri Miyamoto, and Maurício S. Baptista

J. Am. Chem. Soc., **Just Accepted Manuscript** • DOI: 10.1021/jacs.8b05014 • Publication Date (Web): 10 Jul 2018

Photosensitized membrane permeabilization requires contact-dependent reactions between photosensitizer and lipids

Isabel O. L. Bacellar,[†,‡] Maria Cecilia Oliveira,[§] Lucas S. Dantas,[†] Elierge B. Costa,[§] Helena C. Junqueira,[†] Waleska K. Martins,[∥] Andrés M. Durantini,[‡] Gonzalo Cosa,[‡] Paolo Di Mascio,[†] Mark Wainwright,[⊥] Ronei Miotto,[§] Rodrigo M. Cordeiro,[§] Sayuri Miyamoto,[†] Mauricio S. Baptista[†,*]

[†]Departamento de Bioquímica, Instituto de Química, Universidade de São Paulo, Av. Prof. Lineu Prestes 748, São Paulo, SP, Brazil, 05508-000.

[‡]Department of Chemistry and Center for Self-Assembled Chemical Structures CSACS/CRMAA, McGill University, 801 Sherbrook Street West, Montreal, QC, Canada, H3A 0B8.

[§]Centro de Ciências Naturais e Humanas, Universidade Federal do ABC, Avenida dos Estados 5001, Santo André, SP, Brazil, 09210-580.

[∥]Universidade Anhanguera de São Paulo, Av. Raimundo Pereira de Magalhães, 3305, São Paulo, SP, Brazil, 05145-200.

⊥School of Pharmacy & Biomolecular Sciences, Liverpool John Moores University, Liverpool, United Kingdom, L3 3AF.

ABSTRACT: Although the general mechanisms of lipid oxidation are known, the chemical steps through which photosensitizers and light permeabilize lipid membranes are still poorly understood. Herein we characterized the products of lipid photooxidation and their effects on lipid bilayers, also giving insight into their formation pathways. Our experimental system was designed to allow two phenothiazinium-based photosensitizers (methylene blue, MB, and DO15) to deliver the same amount of singlet oxygen molecules per second to 1-palmitoyl-2-oleoyl-*sn*-glycero-3-phosphocholine (POPC) liposome membranes, but with a substantial difference in terms of the extent of direct physical contact with lipid double bonds, *i.e.*, DO15 has a 27-times higher co-localization with ω-9 lipid double bonds than MB. Under this condition, DO15 permeabilizes membranes at least one order of magnitude more efficiently than MB, a result which was also valid for liposomes made of polyunsaturated lipids. Quantification of reaction products uncovered a mixture of phospholipid hydroperoxides, alcohols, ketones and aldehydes. Although both photosensitizers allowed the formation of hydroperoxides, the oxidized products that require direct reactions between photosensitizer and lipids were more prevalent in liposomes oxidized by DO15. Membrane permeabilization was always connected with the presence of lipid aldehydes, which cause a substantial decrease in the Gibbs free energy barrier for water permeation. Processes depending on direct contact between photosensitizers and lipids were revealed to be essential for the progress of lipid oxidation and consequently for aldehyde formation, providing a molecular-level explanation of why membrane binding correlates so well with the cell-killing efficiency of photosensitizers.

INTRODUCTION

Photosensitized oxidations, which are reactions elicited by the interaction of light with a photosensitizer molecule (PS) in the presence of oxygen, have well-known detrimental biological effects (*e.g.* skin aging and cancer[1] and inhibition of photosynthesis[2–4]). Remarkably, medical technologies have also been ingeniously developed for exploiting these reactions to trigger oxidation of biomolecules and consequently to eliminate cancer cells or pathogens[5,6]. Nevertheless, although the general mechanisms of photosensitized oxidations are known[7], the detailed molecular steps leading to biological injury remain largely uncharacterized[8].

Lipid membranes are important targets of photosensitized oxidations[9–14], undergoing several transformations upon lipid photooxidation. Many of these transformations are attributed to lipid hydroperoxides, which have been detected in photooxidized membranes by various techniques (*e.g.*, mass spectrometry, MS)[15–20]. Lipid hydroperoxides, formed as the primary product of the reaction of singlet oxygen ($^1O_2$) with unsaturated lipids (*i.e.*, ene reaction[21]), adopt modified fatty-acyl chain conformations in lipid membranes and lead to lipid lateral phase separation, increase in surface area and decrease in membrane thickness and elastic moduli[10,22]. Yet, the most impacting transformations inflicted on lipid membranes, *i.e.*, those breaking down transmembrane chemical gradients[9,23] (Scheme 1A), remain poorly understood. Although a general scheme of lipid photosensitized oxidation reactions was proposed long ago by Girotti[21] and despite a multitude of studies characterizing biophysical aspects of this phenomenon (*e.g.*, permeabilization rates and transmembrane pore opening)[24–27], there is currently a lack of experimental evidence on the nature of products and elementary steps leading to membrane permeabilization. Unveiling this mechanism is key to minimizing detrimental biological effects of photooxidations[1,2] and to improving technologies based on PSs (*e.g.*, photodynamic therapy, PDT)[6,28].

$^1O_2$ is usually considered to be the most important species involved in photosensitized lipid oxidations. With an average diffusion range of *ca.* 100 nm in water, $^1O_2$ can react with targets that are close to, but not necessarily in direct contact

with PSs[8]. Not surprisingly, given its relatively long action range and high reactivity, most of the efforts on PS development for medical applications have thus focused on enhancing $^1O_2$ generation[8]. However, a number of findings contest the paradigm that a diffusive species (*i.e.* $^1O_2$) is key to causing membrane permeabilization. They rather suggest that contact-dependent reactions with excited states of PSs (*e.g.*, those involving hydrogen or e^- transfer with the biological target) may be needed instead (Scheme 1B). First, amphiphilic PSs, which partition and insert in membranes, were proven to be the most efficient in experimental models ranging from membrane mimetic systems to cancer cells and multicellular organisms[9,13,29,30]. In fact, when Anderson and Krinsky first reported in the 1970's that liposomes could be lysed by photooxidation, they already questioned whether or not $^1O_2$ was the major player in this phenomenon[31]. Second, and contrary to the popular belief that $^1O_2$-derived lipid hydroperoxides permeabilize membranes, there is growing experimental and computational evidence showing that lipid hydroperoxides form stable membranes that sustain chemical gradients[22,32–35]. Third, phospholipid aldehydes bearing truncated fatty-acyl chains have been shown to disrupt chemical gradients when incorporated into membrane mimetic systems and in molecular dynamics simulations[32,34,36–38]. While being a plausible intermediate in membrane permeabilization mechanisms and being a known product of photosensitized oxidations[15], phospholipid aldehydes have yet to be shown to arise *in situ* during photoinduced membrane permeabilization.

Scheme 1. The chemical steps through which photosensitizers (PSs) and light permeabilize lipid membranes are still poorly understood (A), with the relative importance of contact-independent pathways and contact-dependent pathways remaining to be determined (B).

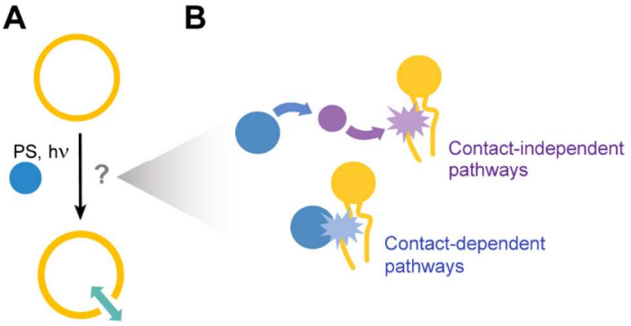

Blue circles represent PSs, while the purple circle represents mainly diffusive $^1O_2$ species. Lipids are represented in gold.

Herein we report experimental and theoretical studies describing the chemical pathway leading to photoinduced membrane permeabilization. In particular, we designed the experiments in order to compare quantitatively the roles that contact independent and contact-dependent processes have in membrane permeabilization.

RESULTS AND DISCUSSION

Membrane permeabilization and the identity of photooxidized lipids. In order to correlate membrane permeabilization with lipid oxidation and propose mechanistic routes, we compared the photoinduced effects of two phenothiazinium dyes: methylene blue (MB) and DO15 (Figure 1A). The two compounds exhibit similar photophysical properties ($^1O_2$ generation quantum yields, Φ_Δ = 0.52 and 0.49 ± 0.02, respectively[39,40]) and are chemically similar, as they are based on the same chromophore, though differing drastically in terms of hydrophobicity (log P = -0.10 and +1.9, respectively[41,42]) and hence in their interaction with membranes and membrane damage efficiency[39]. As model membranes, we employed in most of the experiments liposomes made of 1-palmitoyl-2-oleoyl-*sn*-glycero-3-phosphocholine (POPC), which is a lipid bearing a monounsaturated fatty acid (MUFA). Aiming to dissect the impact of lipid oxidation products formed by $^1O_2$ *vs.* by contact-dependent reactions (Scheme 1B), we propose an experimental design in which both PSs delivered almost the same amount of $^1O_2$ to membranes. This was achieved by balancing the experimental conditions (*e.g.*, irradiation wavelength and PS/lipid ratio) with the membrane proximity of the PS and the average diffusion range of $^1O_2$ within its excited state lifetime, resulting in MB and DO15 delivering *ca.* 160 and 140 $^1O_2$ molecules s^{-1} to the liposome membrane, respectively (see Supporting Information (SI) section 2.3 for calculation details). Indeed, under this experimental condition, the total $^1O_2$ near-infrared luminescence signals coming from MB and DO15 samples confirmed that $^1O_2$ is generated in similar quantities for both dyes (Figure S6). It is also noteworthy that in this condition DO15 has a 27-times higher co-localization with ω-9 lipid double bonds than MB (see SI for calculation details), due to a 21-fold larger number of PS molecules partitioning in the membranes and to a 1.3-fold larger overlap with the intramembrane distribution of the POPC ω-9 double bond (Table S2 and Figure S3).

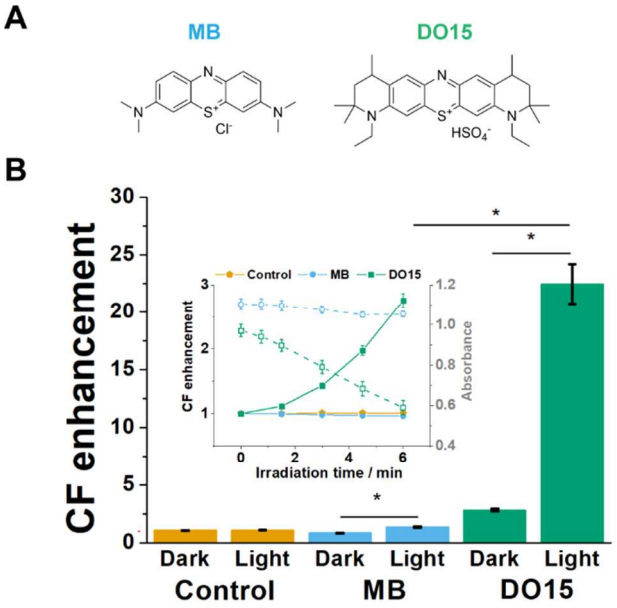

Figure 1. Photosensitized membrane permeabilization by methylene blue (MB) and DO15. (A) Structure of the photosensitizers MB and DO15. (B) Fluorescence enhancement of 5(6)-carboxyfluorescein (CF) encapsulated in POPC liposomes (10 mM Tris 0.3 M NaCl, pH = 8) without PS (controls) or with either MB or DO15 (15 μM), after 120 min in the dark or under light exposure (631 nm, 72 ± 1 W m^{-2}). Inset: CF enhancement kinetics (left axis, filled marks) and absorbance variations (right axis,

empty symbols – MB: 633 nm; DO15 679 nm) for the first 6 min of irradiation. *denotes p-value < 0.05.

Membrane permeabilization assays (Figure 1B, main graph and inset, left axis), based on the leakage of the probe 5(6)-carboxyfluorescein (CF), showed that DO15 permeabilized membranes significantly faster (within minutes) than MB, and that membrane permeabilization was accompanied by a significant decrease in the absorbance of the dye (inset, right axis). Although DO15 is ~16-fold more efficient than MB in terms of the kinetics of membrane permeabilization as a function of irradiation time, after 120 min both dyes led to significant liposome permeabilization. It is important to mention that neither DO15 in the absence of light (dark, Figure 1B and Figure S7) nor its bleached species (Figure S7) cause membrane permeabilization. In addition, the chelator DTPA did not affect the permeabilization kinetics, ruling out a possible dependence on trace metals (Figure S8). The higher efficiency of DO15 to permeabilize membranes adds to a general trend of membrane permeabilization and PS efficiency being associated with membrane binding, observed for these same PSs in other membrane models[39] and for other classes of PSs in other experimental models[9,13,29,30]. This tendency becomes quantitative in our experimental design, in which fluxes of $^1O_2$ molecules reaching the membrane are almost the same, and the level of triplet excited states diffusing from the aqueous solution and reaching the membrane is twice as large for MB than for DO15 (see SI for details). Indeed, permeabilization seems to correlate well with the number of triplets generated within the membrane that co-localize with lipid double bonds, which is 13 times larger for DO15 than for MB (see SI, section 2.3), suggesting a significant contribution of contact-dependent reactions to the formation of oxidized lipids.

While our PSs and lipid were selected to facilitate mechanistic studies, with the choice for a monounsaturated lipid (POPC) to prevent competition from auto-oxidation processes, we understand that it is critical to test whether or not these results also apply for different membrane compositions, including lipid mixtures. Specifically, lipids bearing polyunsaturated fatty acids (PUFAs) are important components of membranes and, by having bis-allylic hydrogens, they display a substantially lower energy barrier for the rate-limiting H-atom abstraction step of peroxidation propagation. To verify if the distinct behavior of DO15 and MB also applies to PUFA phospholipids, we tested how liposomes made of 1-palmitoyl-2-arachidonoyl-*sn*-glycero-3-phosphocholine (PAPC) respond when challenged with MB and DO15 under the same experimental condition as described in Figure 1. Figure S9 shows that the efficiency ratio between MB and DO15 is maintained when oleyl chains are replaced by arachidonoyl, suggesting that the same kind of mechanism operates under both conditions. Even though PAPC favors radical-mediated autooxidation pathways, it also reacts faster than POPC with both triplet states and $^1O_2$[21,43–45] (see further discussion below).

HPLC-MS/MS studies of photooxidized liposomes revealed three major oxidation products: lipid hydroperoxides (*m/z* 792.6), alcohols (*m/z* 776.6) and ketones (*m/z* 774.6) (Figure 2A-B, see also Figure 2C for formation kinetics and the SI for additional details). While hydroperoxides were the main products for both PSs, DO15 led to more hydroperoxides than MB (45 ± 2 μM and 13 ± 2 μM, respectively, corresponding to 10 ± 1 % and 2.7 ± 0.1 % of the initial POPC concentration), and also to a *ca.* 4.5-fold higher concentration of total oxidized lipids (*ca.* 60 μM). Alcohols and ketones, which were formed in smaller quantities than hydroperoxides, totalizing *ca.* 17 μM and 1 μM for DO15 and MB, respectively (*ca.* 4 % and 0.2 % of the initial POPC concentration), were also quantified directly from the reaction mixture. Both classes of oxidized lipids had been previously described to be products of photosensitized oxidations, but never quantified during the course of membrane permeabilization[16,46]. Our observation that alcohols and ketones occur in equimolar proportions (p-value = 1.000) suggests that they are produced via the Russell mechanism (Scheme 2 – step 4), which is based on the decomposition of a tetroxide intermediate formed upon combination of two peroxyl radicals[47,48].

Since our analysis focused mainly on the initial steps of membrane photooxidation, we expected that truncated phospholipids bearing oxidized moieties (aldehydes and carboxylic acids[23]) could be present in the studied samples in very low concentration at this stage. In order to enable the detection of these compounds even at low levels, we resorted to their derivatization with the probe 1-pyrenebutyric hydrazide (PBH, see Figure 3A and Figure S13 for adduct structures)[49,50], followed by analysis by HPLC-MS/MS (Figure 3B, see also SI for additional details). Addition of this probe to photooxidized liposomes revealed the formation of phospholipid aldehydes but not of carboxylic acid derivatives. Truncated phospholipid aldehydes with different chain lengths were observed (*m/z* 920.5546, 934.5695 and 946.5700, corresponding to 8-, 9- and 10-carbon chains, respectively) (Figure 3A) and, most importantly, only in those samples that also suffered membrane permeabilization. Liposomes treated with DO15 were permeabilized within minutes of irradiation, showing a significant increase in the amount of aldehydes on this timescale (~ 2 μM, Figure 3C). In turn, during the initial steps of irradiation, MB did not permeabilize membranes and did not form aldehydes. However, prolonged irradiation (120 min) of MB ultimately led to membrane permeabilization to the same extent as DO15 (compare to 3 min of irradiation, when both samples show CF emission enhancement of *ca.* 1.4, see Figure 1B). Remarkably, aldehydes were detected in these samples at concentrations similar to those found in samples irradiated for a 40-fold shorter period with DO15 (Figure 3D, p-value = 0.119), supporting the view that aldehydes are the products that cause membrane permeabilization. These results are the first that definitively associate membrane permeabilization with *in situ* aldehyde generation and accumulation.

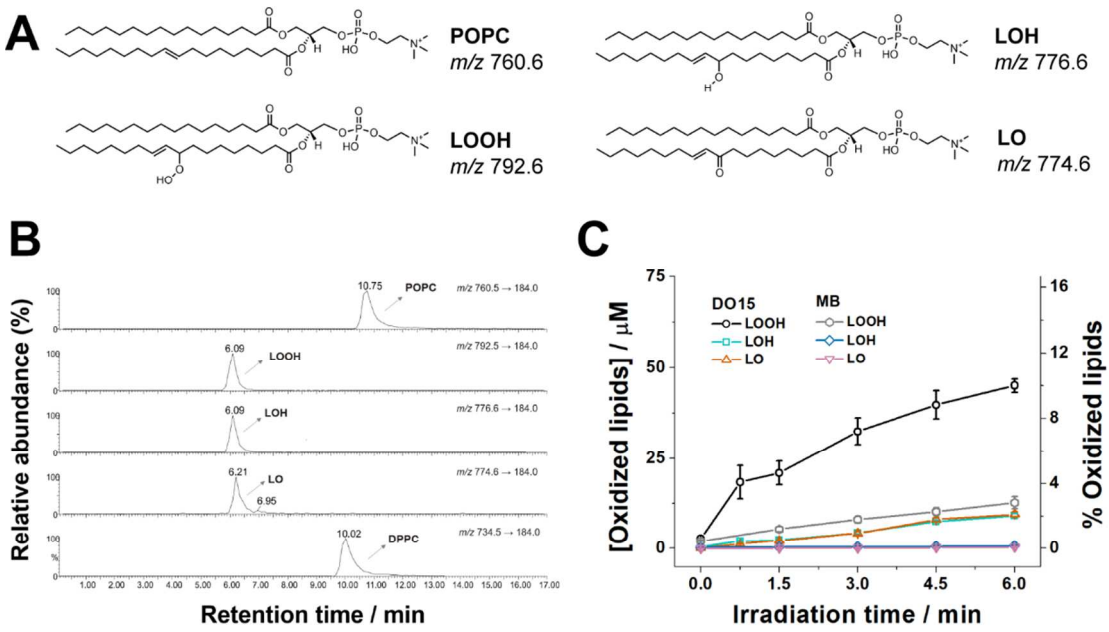

Figure 2. Oxidized lipids detected during photooxidation of POPC liposomes. (A) Structures and *m/z* for the $[M+H]^+$ ions detected for POPC and its major oxidation products: hydroperoxides (LOOH), alcohols (LOH) and ketones (LO), represented here by the 9-E isomers. (B) Multiple reaction monitoring (MRM) chromatograms for each of the transitions $[M+H]^+ \rightarrow$ *m/z* 184.0, in ESI+ mode; DPPC was employed as internal standard. (C) Concentration of oxidized lipids in μM (left) and in percentage of the initial POPC concentration (right) as a function of irradiation time (631 nm, 72 ± 1 W m^{-2}). [PS] = 15 μM.

Scheme 2. Chemical pathways for photoinduced membrane permeabilization. The map distinguishes between contact-independent and contact-dependent processes, which rely on $^1O_2$ or on direct reactions between PSs and lipids, respectively.

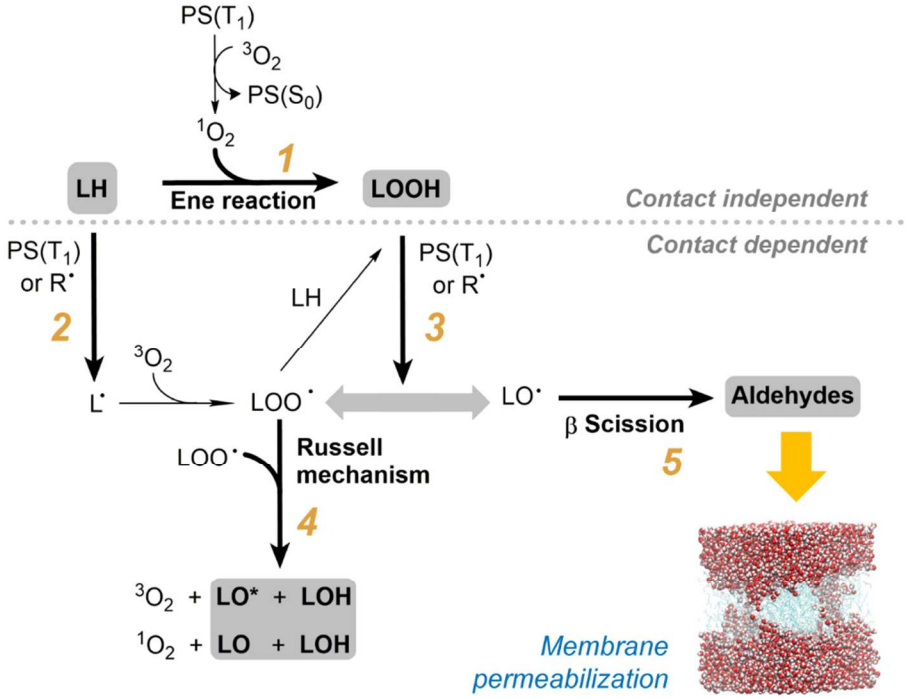

$PS(S_0)$, $PS(T_1)$: PS ground and excited triplet states; $^3O_2$,$^1O_2$: ground and excited singlet states of oxygen; $R^\bullet$: generic radical species; LH: non-oxidized lipid; $L^\bullet$, $LOO^\bullet$, $LO^\bullet$: lipid carbon-centered, peroxyl and alkoxyl radicals; LOOH, LOH, LO, LO^*: lipid hydroperoxide, alcohol, ketone and excited state ketone. A snapshot of a simulated aldehyde membrane, showing pore opening, is also provided.

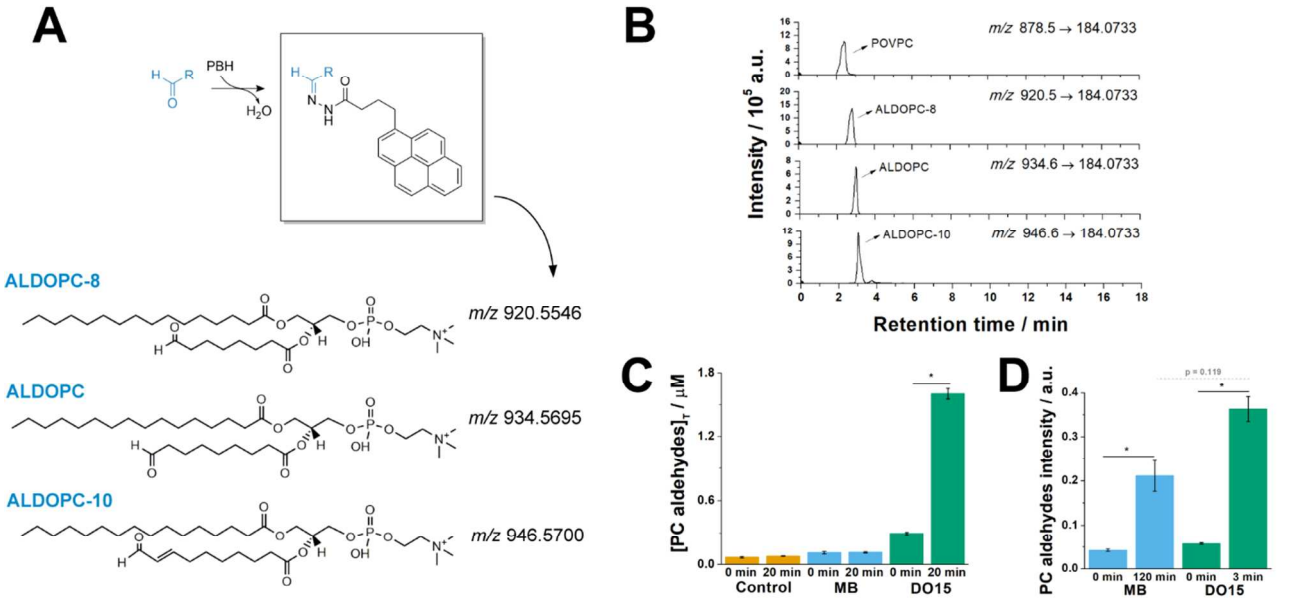

Figure 3. Quantification of POPC-derived aldehydes. (A) Structures of POPC-derived phospholipid aldehydes (ALDOPC-8, ALDOPC and ALDOPC9) and *m/z* for the respective $[M+H]^+$ ions. Aldehydes were detected as PBH adducts, as represented above. (B) Parallel reaction monitoring (PRM) chromatograms for each of the transitions $[M+H]^+ \rightarrow m/z$ 184.0733, in ESI+ mode (POVPC: 1-palmitoyl-2-(5'-oxo-valeroyl)-*sn*-glycero-3-phosphocholine, employed as internal standard). Samples consisted of POPC liposomes irradiated (631 nm, 72 ± 1 W m^{-2}) for 20 min with DO15. (C) Total aldehyde concentration at 0 and 20 min of irradiation without (control) or with PSs. (D) Comparative quantification of total aldehydes at 0 min and at 120 min of irradiation with MB or at 3 min of irradiation with DO15. [PS] = 15 μM. [POPC] was 2.5-fold lower in (C), being the same as for Figure 2, see SI for details. *denotes p-value < 0.05.

The effects of photooxidized lipids.

In the absence of protein channels, transmembrane solute permeation may follow two mechanisms: solubility-diffusion or pore-mediated translocation. The permeation of small, electrically neutral molecules can be explained by the solubility-diffusion model[51], while permeation of ionic species is usually explained by the formation by thermal fluctuations of membrane-spanning transient pores, which allow ions to retain at least part of their hydration shell as they cross the membrane[52,53]. Pore-mediated ionic permeation is strongly dependent on the membrane thickness[54,55] and is favored by decreases in lipid packing[56].

The phenomenon of oxidatively-induced membrane permeabilization can also be rationalized under the premises of these mechanisms. Lipid oxidation gives rise to hydrophilic functional groups along the lipid acyl chains. These groups reside close to the membrane surface, but due to thermal motions, they are broadly distributed and are also able to populate the membrane interior[35]. Our simulations revealed that the presence of hydroperoxide and alcohol functional groups did not significantly change the permeation free energy barrier of water, although increasing the area per lipid and decreasing membrane thickness (Figure S16 and Table S4). Table 1 shows the calculated free energy barriers of water permeation through pristine POPC and all the simulated fully oxidized bilayers, thus providing a quantitative comparison of water permeability for the different classes of oxidized lipids. Membranes made of hydroperoxides, alcohols and ketones posed similar or higher permeation barriers as POPC (~30 kJ mol^{-1}). This indeed explains why massively hydroperoxidized membranes are still stable and functional as permeation barriers (Figure 4A, Figure S16A and [35]). These trends are supported by other simulations of permeation of hydrophilic molecules through phospholipid hydroperoxide membranes[33].

A completely different scenario emerges in the case of truncated-chain phospholipid aldehydes, which led to a much thinner membrane (Table 4) and also to a more than 2-fold decrease in the energy barrier for water permeation, mainly due to the formation of transmembrane pores. This result is clearly seen in Figure 4D-E, where aldehyde groups span the whole membrane (D), while water molecules permeate across the bilayer (E). The pore is stable for hundreds of nanoseconds, until the end of the simulation. Other simulations showed that sparsely distributed aldehydes clump together and facilitate water permeation by a shuttling mechanism, in which the polar groups of aldehydes pull water molecules into the bilayer[32]. Therefore, permeabilization can happen as lipid aldehydes begin to be formed.

The fact that aldehydes increase membrane permeability at low concentrations was also shown by assembling membranes with commercially available aldehydes. For instance, when Ytzhak and Ehrenberg studied the permeabilization effects of ALDOPC and a shorter chain phospholipid aldehyde in egg lecithin liposomes, they observed dissipation of an ionic gradient by employing as little as 2% of any of these aldehyde species, with higher concentrations amplifying this effect[38]. By working with GUVs containing cholesterol and saturated and unsaturated lipids, Runas *et al*. observed that increasing the amount of ALDOPC from 0 to 2.5% enhanced by one order of magnitude membrane permeability to a fluorescent, short-chain poly(ethylene glycol) molecule (PEG12-NBD)[36]. Therefore, our results (Figure 3D) confirmed the hypothesis that aldehydes cause membrane permeabilization, which is also compatible with previous work performed by others[32,57].

Table 1. Gibbs free energy barrier for water permeation through simulated single-component membranes.

	POPC	LOOH	LOH	LO	ALDOPC
ΔG / kJ mol^{-1}	31 ± 3	30 ± 5	30.0 ± 0.3	> 34	12 ± 4

LOOH, LOH, LO, ALDOPC: POPC-derived hydroperoxide, alcohol, ketone and aldehyde, respectively. See SI for calculation details.

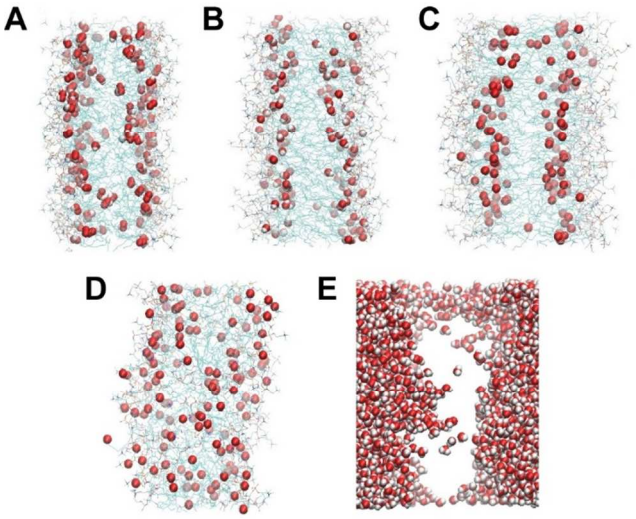

Figure 4. Snapshots from molecular dynamics simulations of oxidized lipid membranes. Single-component membranes were composed of POPC-derived (A) hydroperoxides, (B) alcohols, (C) ketones or (D-E) aldehydes, with the oxidized groups highlighted in red (van der Waals spheres) for A-D. Water molecules were omitted for simplicity, except for (E), in which lipids were omitted instead.

The mechanism of membrane permeation by aldehyde-bearing truncated phospholipids does not seem to apply to other phospholipids bearing shorter alkyl chains. For example, truncated lipids bearing a carboxylic acid contribute to the increase in the disorder of the hydrophobic region of the bilayer, but not enough to lead to pore formation[58], in marked contrast to aldehydes. Besides, our experiments did not show the presence of truncated lipids bearing carboxylic acids in the initial steps of photooxidation, in a timeframe that membranes are already permeabilized in the presence of aldehyde-bearing truncated phospholipids. Another interesting result was obtained by Ytzhak and Ehrenberg, who observed that incorporation of L-α-lysophosphatidylcholine to liposomes did not cause dissipation of ionic gradients at concentrations in which phospholipid aldehydes did[38].

While hydroperoxides, alcohols and ketones were formed in larger concentration than aldehydes (1.6 ± 0.2 μM after 6 min of irradiation with DO15, *i.e.* ~6-fold smaller than that of alcohols or ketones), only the latter significantly favored water permeation and led to pore opening. Through quantification of multiple lipid oxidation products in different stages of the membrane permeabilization process, we demonstrated that membrane permeabilization correlates with phospholipid aldehyde detection; this is especially evident when we compare samples irradiated with MB for shorter times, when no permeabilization is seen and no aldehydes are detected, *versus* samples irradiated for longer times, when both permeabilization and aldehyde levels are significant. DO15 shows much faster permeabilization kinetics and, indeed, aldehydes can be detected much earlier than for MB. We are thus confident that these theoretical and experimental evidences clearly converge to prove the crucial role of aldehydes in photoinduced membrane permeabilization.

Sources of photooxidized lipids. Understanding the pathways (Scheme 2) behind lipid photooxidation is mandatory in order to control membrane permeabilization, which in a biological scenario ultimately determines the option between programed cell death pathways or accidental cell death[8,9]. Photosensitized oxidations encompass both direct reactions between PSs and substrates (*e.g.*, lipids) and reactions depending on a mediating species, most often $^1O_2$. We set up experimental conditions in which DO15 and MB delivered similar amounts of $^1O_2$ to membranes. Even then, DO15 had a higher photooxidation efficiency, which suggests that contact-dependent PS-lipid reactions have a key role. This is further supported by the detection of alcohol and ketones, which not only are not expected from $^1O_2$ chemistry alone but were also formed in proportions consistent with peroxyl radicals being their precursor (Scheme 2 – step 4). Further support for the key role of radical-mediated pathways was provided by the detection of phospholipid aldehydes, as further discussed below.

The initiation and progress of radical-mediated lipid oxidation in the absence of metals relies on contact-dependent reactions of the triplet excited state of PSs, which are prone to abstract hydrogens or donate electrons[7]. Possible targets of triplets are double bonds (H-abstraction) and/or hydroperoxides (electron donation), which can be made available in the membrane by parallel ene reaction[59] (Scheme 2 – steps 2, 3). Figure 1B (inset, right axis) shows that membrane permeabilization is invariably coupled to PS bleaching, as characterized by a decrease in the main absorption band of the PSs (630-680 nm). This is consistent with the direct involvement of the PS in contact-dependent reactions with lipids. Indeed, spectral changes observed during irradiation confirmed that DO15 extensively bleaches during membrane permeabilization experiments (Figure 5A-C and Figure S17). Moreover, the photobleaching rates of DO15 paralleled the rate of absorption increase at *ca.* 225 nm, which corresponds to the formation of lipids bearing α,β-unsaturated ketones[60] (Figure 5D, see also Figure S10). Compared with a water control, both the photobleaching rate of DO15 (Figure 5B-C) and the consecutive formation of oxidized lipids (Figure 5D) increased in the presence of lipids bearing allylic hydrogens (POPC and 1,2-dioleoyl-*sn*-glycero-3-phosphocholine, DOPC) or hydroperoxides, but not in the presence of saturated lipids (1,2-dipalmitoyl-*sn*-glycero-3-phosphocholine, DPPC). Even though photobleaching rates are very similar in pure POPC and DOPC membranes, experiments carried out in membranes containing a saturated lipid and smaller percentages of POPC or DOPC showed that the photobleaching rates indeed depended on the concentration of double bonds (Figure S18). Yet, in pure unsaturated lipid bilayers the rates converge due to a saturation effect of the double bond concentration. The increase in DO15 photobleaching by unsaturated lipids

demonstrates the significance of the abstraction of allylic hydrogens by the PS. These reactions yield lipid carbon-centered radicals, which rapidly react with oxygen and form peroxyl radicals[61], contributing to the buildup of the peroxyl radical pool from which alcohols and ketones arise. Importantly, the photobleaching rates of MB were shown to be poorly dependent on liposome composition or even on their presence (Figure 5B), in accordance with the higher hydrophilicity and lower membrane permeabilization efficiency of MB.

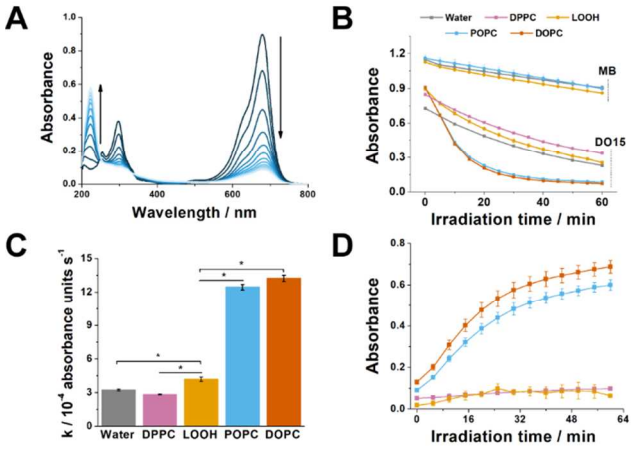

Figure 5. Spectral changes observed upon irradiation of PSs in the presence of liposomes. (A) Absorption spectra of DO15 (15 μM) in the presence of POPC liposomes at different irradiation times (650 nm, 35 mW, 5 min intervals). (B) Change in the absorbance of the main absorption band of DO15 (graph A, downward arrow) during irradiation in the absence or in the presence of DPPC, POPC hydroperoxides (LOOH), POPC and DOPC liposomes. Data is also provided for MB (15 μM) in water, liposomes of POPC and LOOH. (C) Photobleaching rate constants for DO15, obtained from (B). (D) Change in the absorbance in the ketone absorption band (graph A, upward arrow) of liposomes irradiated in the presence of DO15, under the same conditions as in (B). *denotes p-value < 0.05.

Previous reports showed that hydroperoxides quench the excited triplet state of MB, while also suggesting that this reaction forms alkoxyl radicals[62,63]. The fact that the photolysis of DO15 in the presence of POPC hydroperoxide liposomes indeed showed an increase in dye bleaching rates if compared with photolysis in water (Figure 5C and Figure S17) supports the hypothesis that DO15 can also directly produce peroxyl and/or alkoxyl radicals by reacting with hydroperoxides (Scheme 2 – step 3). We highlight that not all -OOH groups of hydroperoxide are localized at the membrane/water interface and some may be closer to the original position of lipid unsaturation (Figure 4A, see also [35]); therefore, the distribution of DO15 in the membrane would likely overlap with the distribution of -OOH groups. The hypothesis that DO15 generates oxygenated lipid radicals was confirmed by irradiating liposomes containing DO15 and the fluorogenic probe H_2B-PMHC, which is an α-tocopherol analogue whose fluorescence is enhanced upon reaction with peroxyl or alkoxyl radicals[64] (Figure S19). Not only did significant enhancement of H_2B-PMHC's fluorescence occur in the presence of oxygen (Figure 6A), but also enhancement rates were higher in water than in deuterium oxide (Figure 6B). We highlight that these results follow the opposite trend expected for any $^1O_2$-dependent process, due to the longer lifetime of $^1O_2$ in D_2O. Instead, this isotopic effect can be associated to the fact that -OOH/D groups engage in proton exchange[65]: the substitution of hydrogen by deuterium would lower the rates of H-/D-atom abstraction by the triplet excited state of DO15, thus decreasing the enhancement rate of H_2B-PMHC. On the same line, the reaction of H_2B-PMHC in the presence of alkoxyl or peroxyl radicals involves H-atom abstraction from the chromanol trap segment, where kinetic isotope effect (KIE) can be invoked in going from H_2O to D_2O as has been shown for tocopherol[66–69] and the first generation fluorogenic antioxidant probe B-TOH[69]. Therefore, our results imply that oxygenated lipid radicals generated through contact-dependent reactions are involved in lipid membrane photooxidation.

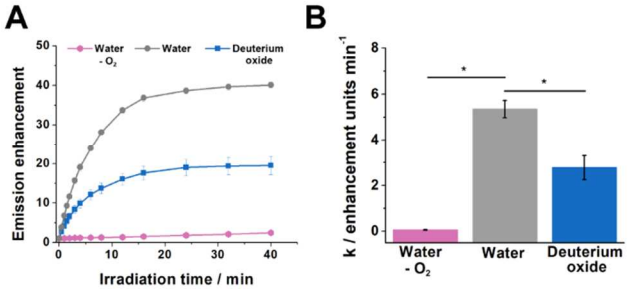

Figure 6. Detection of lipid oxygenated radicals by the fluorogenic probe H_2B-PMHC. Fluorescence enhancement (A) kinetics and (B) rate constants for H_2B-PMHC in POPC liposomes. Samples were irradiated (634 nm, 1.85 mW cm^{-2}) with DO15 (0.24 μM) in water (argon purged or air-equilibrated) or deuterium oxide-based PBS. *denotes p-value < 0.05.

We finally consider the main reaction that leads to formation of lipid aldehydes in our system, which can be produced either through radical-mediated reactions or through hydroperoxide decomposition, *i.e.*, presumably directly from $^1O_2$ products and without the need of contact-dependent processes. In the case of monounsaturated lipids, these processes correspond, respectively, to alkoxyl radical β-scission (Scheme 2 – step 5 and Scheme 3B) and hydroperoxide Hock cleavage (Scheme 3A)[70,71].

Scheme 3. Possible reactions leading to phospholipid aldehydes and membrane permeabilization. (A) Hydroperoxide Hock cleavage and (B) alkoxyl radical β-scission, for related hydroperoxide and alkoxyl radical structures.

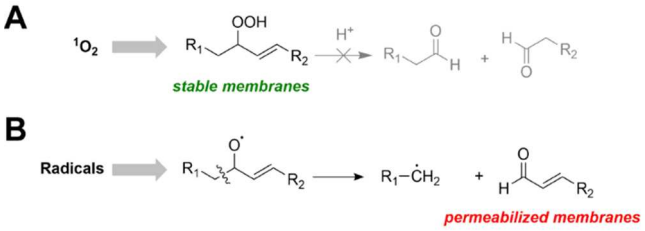

Hock cleavage, though never demonstrated for monounsaturated phospholipids, is commonly proposed as a source of aldehydes directly from other classes of hydroperoxides[23,27,72]. Still, the conditions in which Hock cleavage was shown to occur were invariably either in organic solvents or in thin films of lipids exposed to an undefined atmosphere, usually

with an unknown amount of acid added to the sample. Consequently, the role of Hock cleavage under biologically-relevant conditions remains controversial. Indeed, some works (*e.g.*, by Morita's group) suggest that steps involving radicals may be required instead[73]. Nonetheless, this mechanism is still frequently mentioned to explain peroxidation progression in membranes as a subsequent step of hydroperoxide formation. Our data indeed show that hydroperoxides will persist in lipid membranes, even in conditions that could, in principle, catalyze Hock cleavage. We observed that giant unilamellar vesicles (GUVs) made of POPC hydroperoxides remained impermeable to sugars independent of pH, similar to GUVs made of pristine POPC (Figure S20). The fact that membranes retained their impermeability even at pH 3.5 discards the acid-catalyzed Hock cleavage as a pathway for phospholipid aldehyde formation under the conditions studied. Not even membranes made of lipids having a polyunsaturated chain, *i.e.*, PAPC and its hydroperoxides, showed any pH-dependent permeabilization effect. In addition to that, neither POPC hydroperoxides nor PAPC hydroperoxides GUVs were permeabilized by adding a Lewis-acid (Fe(III) salt). Note also that this GUV assay is a sensitive measure of membrane permeabilization, as POPC hydroperoxides and PAPC hydroperoxides GUVs are permeabilized within minutes of exposure to Fe(II), showing that the experimental system responds positively to radical type (Fenton reaction) oxidative damage in the membrane (Figure S21). Moreover, Hock cleavage of POPC hydroperoxides would only yield aldehydes bearing saturated carbon chains, while one of the aldehyde species detected had a 10-carbon monounsaturated chain (Figure 3A). The formation of this product, together with the other two species detected (with 8 and 9-carbon saturated chains), is consistent with alkoxyl radical β-scission (Scheme 2 – step 5, see also SI for details – Figure S22), a pathway relying on radical chemistry and consistent with the production of oxygenated radicals by DO15 and with their role in lipid peroxidation propagation[70,74]. Therefore, our experiments provide further evidence that lipid hydroperoxides do not suffer direct scission by Hock cleavage, supporting the need for direct-contact reactions that lead to the formation of radicals that ultimately yield truncated aldehydes via alkoxyl radical β-scission. These, in turn, initiate membrane permeabilization, as summarized in Schemes 2 and 3. The permeabilization experiment performed with PAPC liposomes (Figure S9), as well as previously-reported permeabilization experiments carried out with soy-lecithin liposomes (containing 39% of PUFAs)[39], provides evidence that contact-dependent pathways are also important for membranes made of PUFA lipids. Since the timeframe of the photoinduced processes is a lot shorter than that of the autooxidation processes, the contact-dependent reactions, which govern photoinduced permeabilization in membranes bearing only MUFAs, also seem to be governing permeabilization of membranes bearing PUFAs. Thus, these results suggest that the findings reported herein and the proposed chemical pathway can be extended to other lipid compositions.

The original definition of type I and type II photooxidations by Foote has emphasized the contrast between processes depending on direct contact between PSs and substrates or alternatively relying on diffusive, reactive species[7,75]. Hence, our data explain the key role of contact-dependent pathways for improving photodynamic efficiency, and suggest that the efficacy of PSs can be considerably improved by targeting for direct reactions and expanding their action mechanism beyond $^1O_2$ generation[76]. Interestingly, natural PSs such as flavin and pterins also seem to oxidize biological substrates preferentially through contact-dependent reactions[44,77,78]. We envisage several implications of this knowledge. For example, since membrane permeabilization depends on redox reactions, which are likely to cause PS bleaching, finding novel ways to regenerate PSs would allow the design of better photosensitizing agents. Likewise, in order to either increase or avoid damage induced by photosensitized oxidations, one can respectively try to increase or avoid accumulation of lipid aldehydes.

CONCLUSIONS

The involvement of carbon-centered, alkoxyl and peroxyl lipid radicals in the progression of lipid peroxidation is a well-known fact[21,61]. However, the specific details of how these species are actually formed during photosensitized oxidations and ultimately lead to membrane permeabilization has remained elusive. By comparing two PSs with similar intrinsic photophysical and photochemical properties, but differing in terms of membrane permeabilization efficiencies, we showed that membrane permeabilization is associated with aldehyde production, which can only occur when there are direct reactions between the excited triplet state of the PS and the major targets in the lipid membrane, *i.e.*, lipid unsaturation and -OOH groups formed after the initial ene reaction with $^1O_2$. These results, as well as the major reactions operating during membrane photooxidation, are summarized in Scheme 2. The role of contact-dependent processes in biological photooxidations is often considered secondary to $^1O_2$-mediated oxidations, and consequently $^1O_2$ production is usually the main parameter considered for the development of new PSs. However, our results demonstrate that, for a PS to fully compromise membrane function, it needs to be sacrificed through contact-dependent reactions. Therefore, activation/suppression of PS regeneration could be explored as an effective tool to maximize or counter the effects of photosensitized oxidations. We are confident that the roadmap presented herein will provide mechanistic guidelines for further developments in photomedicine and photoprotection. Moreover, we hope that our work will stimulate studies with more complex lipid compositions, as well as studies aiming to understand in more detail cell death pathways that depend on lipid oxidation, such as ferroptosis[79]. We also foresee that, since membrane damage will depend on the molecular contact between the PS and the lipid, and not so much on diffusive species, one may start to develop efficient photoinduced organelle-depletion methods[9].

ASSOCIATED CONTENT

Supporting Information. Computational and experimental methods, additional data for membrane permeabilization, binding, oxidized lipid analysis, photobleaching, H_2B-PMHC activation pathway, giant unilamellar vesicle permeability and molecular dynamics simulations. This material is available free of charge via the Internet at http://pubs.acs.org.

AUTHOR INFORMATION

Corresponding Author

*baptista@iq.usp.br

Notes

The authors declare no competing financial interests.

ACKNOWLEDGMENT

Fundação de Amparo à Pesquisa do Estado de São Paulo (FAPESP) is acknowledged for financial support (grants 2012/50680-5 and 2013/07937-8 – CEPID Redoxoma). Authors also acknowledge Núcleo de Apoio à Pesquisa em Tecnologia Fotoquímica (NAP-Phototech) and individual FAPESP fellowships (2013/11640-0 and 2015/22935-7). Fernanda M. Prado is acknowledged for assisting some of the HPLC-MS analyses and prof. Frank H. Quina (IQUSP) for revising the manuscript.

REFERENCES

(1) Sander, C. S.; Hamm, F.; Elsner, P.; Thiele, J. J. Oxidative Stress in Malignant Melanoma and Non-Melanoma Skin Cancer. *Br. J. Dermatol.* **2003**, *148* (5), 913–922.

(2) Aro, E.-M.; Virgin, I.; Andersson, B. Photoinhibition of Photosystem II. Inactivation, Protein Damage and Turnover. *Biochim. Biophys. Acta - Bioenerg.* **1993**, *1143* (2), 113–134.

(3) Anthony, J. R.; Warczak, K. L.; Donohue, T. J. A Transcriptional Response to Singlet Oxygen, a Toxic Byproduct of Photosynthesis. *Proc. Natl. Acad. Sci.* **2005**, *102* (18), 6502–6507.

(4) Triantaphylides, C.; Krischke, M.; Hoeberichts, F. A.; Ksas, B.; Gresser, G.; Havaux, M.; Van Breusegem, F.; Mueller, M. J. Singlet Oxygen Is the Major Reactive Oxygen Species Involved in Photooxidative Damage to Plants. *Plant Physiol.* **2008**, *148* (2), 960–968.

(5) Castano, A. P.; Demidova, T. N.; Hamblin, M. R. Mechanisms in Photodynamic Therapy: Part Two - Cellular Signaling, Cell Metabolism and Modes of Cell Death. *Photodiagnosis Photodyn. Ther.* **2005**, *2* (1), 1–23.

(6) Dolmans, D. E. J. G. J.; Fukumura, D.; Jain, R. K. Photodynamic Therapy for Cancer. *Nat. Rev. Cancer* **2003**, *3*, 380–387.

(7) Baptista, M. S.; Cadet, J.; Di Mascio, P.; Ghogare, A. A.; Greer, A.; Hamblin, M. R.; Lorente, C.; Nunez, S. C.; Ribeiro, M. S.; Thomas, A. H.; Vignoni, M.; Yoshimura, T. M. Type I and Type II Photosensitized Oxidation Reactions: Guidelines and Mechanistic Pathways. *Photochem. Photobiol.* **2017**, *93* (4), 912–919.

(8) Bacellar, I. O. L.; Tsubone, T.; Pavani, C.; Baptista, M. Photodynamic Efficiency: From Molecular Photochemistry to Cell Death. *Int. J. Mol. Sci.* **2015**, *16* (9), 20523–20559.

(9) Tsubone, T. M.; Martins, W. K.; Pavani, C.; Junqueira, H. C.; Itri, R.; Baptista, M. S. Enhanced Efficiency of Cell Death by Lysosome-Specific Photodamage. *Sci. Rep.* **2017**, *7* (1), 6734.

(10) Itri, R.; Junqueira, H. C.; Mertins, O.; Baptista, M. S. Membrane Changes under Oxidative Stress: The Impact of Oxidized Lipids. *Biophys. Rev.* **2014**, *6* (1), 47–61.

(11) Sonoike, K. Various Aspects of Inhibition of Photosynthesis under Light/Chilling Stress: "Photoinhibition at Chilling Temperatures" versus "Chilling Damage in the Light." *J. Plant Res.* **1998**, *111* (1), 121–129.

(12) Labuza, T. P.; Dugan, L. R. Kinetics of Lipid Oxidation in Foods. *C R C Crit. Rev. Food Technol.* **1971**, *2* (3), 355–405.

(13) Xu, S.; Chisholm, A. D. Highly Efficient Optogenetic Cell Ablation in C. Elegans Using Membrane-Targeted MiniSOG. *Sci. Rep.* **2016**, *6* (1), 21271.

(14) Roqueiro, G.; Facorro, G. B.; Huarte, M. G.; Rubín de Celis, E.; García, F.; Maldonado, S.; Maroder, H. Effects of Photooxidation on Membrane Integrity in Salix Nigra Seeds. *Ann. Bot.* **2010**, *105* (6), 1027–1034.

(15) Thomas, A. H.; Catalá, Á.; Vignoni, M. Soybean Phosphatidylcholine Liposomes as Model Membranes to Study Lipid Peroxidation Photoinduced by Pterin. *Biochim. Biophys. Acta - Biomembr.* **2016**, *1858* (1), 139–145.

(16) Melo, T.; Santos, N.; Lopes, D.; Alves, E.; Maciel, E.; Faustino, M. A. F.; Tomé, J. P. C.; Neves, M. G. P. M. S.; Almeida, A.; Domingues, P.; Segundo, M. A.; Domingues, M. R. M. Photosensitized Oxidation of Phosphatidylethanolamines Monitored by Electrospray Tandem Mass Spectrometry. *J. Mass Spectrom.* **2013**, *48* (12), 1357–1365.

(17) Wolnicka-Glubisz, A.; Lukasik, M.; Pawlak, A.; Wielgus, A.; Niziolek-Kierecka, M.; Sarna, T. Peroxidation of Lipids in Liposomal Membranes of Different Composition Photosensitized by Chlorpromazine. *Photochem. Photobiol. Sci.* **2009**, *8* (2), 241–247.

(18) Rodriguez, M. E.; Kim, J.; Delos Santos, G. B.; Azizuddin, K.; Berlin, J.; Anderson, V. E.; Kenney, M. E.; Oleinick, N. L. Binding to and Photo-Oxidation of Cardiolipin by the Phthalocyanine Photosensitizer Pc 4. *J. Biomed. Opt.* **2010**, *15* (5), 051604.

(19) Kim, J.; Minkler, P. E.; Salomon, R. G.; Anderson, V. E.; Hoppel, C. L. Cardiolipin: Characterization of Distinct Oxidized Molecular Species. *J. Lipid Res.* **2011**, *52* (1), 125–135.

(20) Kim, J.; Fujioka, H.; Oleinick, N. L.; Anderson, V. E. Photosensitization of Intact Heart Mitochondria by the Phthalocyanine Pc 4: Correlation of Structural and Functional Deficits with Cytochrome c Release. *Free Radic. Biol. Med.* **2010**, *49* (5), 726–732.

(21) Girotti, A. W. Photosensitized Oxidation of Membrane Lipids: Reaction Pathways, Cytotoxic Effects, and Cytoprotective Mechanisms. *J. Photochem. Photobiol. B Biol.* **2001**, *63* (1–3), 103–113.

(22) Weber, G.; Charitat, T.; Baptista, M. S.; Uchoa, A. F.; Pavani, C.; Junqueira, H. C.; Guo, Y.; Baulin, V. A.; Itri, R.; Marques, C. M.; Schroder, A. P. Lipid Oxidation Induces Structural Changes in Biomimetic Membranes. *Soft Matter* **2014**, *10* (24), 4241–4247.

(23) Caetano, W.; Haddad, P. S.; Itri, R.; Severino, D.; Vieira, V. C.; Baptista, M. S.; Schröder, A. P.; Marques, C. M. Photo-Induced Destruction of Giant Vesicles in Methylene Blue Solutions. *Langmuir* **2007**, *23* (3), 1307–1314.

(24) Mertins, O.; Bacellar, I. O. L.; Thalmann, F.; Marques, C. M.; Baptista, M. S.; Itri, R. Physical Damage on Giant Vesicles Membrane as a Result of Methylene Blue Photoirradiation. *Biophys. J.* **2014**, *106* (1), 162–171.

(25) Heuvingh, J.; Bonneau, S. Asymmetric Oxidation of Giant Vesicles Triggers Curvature-Associated Shape Transition and Permeabilization. *Biophys. J.* **2009**, *97* (11), 2904–2912.

(26) Kerdous, R.; Heuvingh, J.; Bonneau, S. Photo-Dynamic Induction of Oxidative Stress within Cholesterol-Containing Membranes: Shape Transitions and Permeabilization. *Biochim. Biophys. Acta* **2011**, *1801*, 2965–2972.

(27) Sankhagowit, S.; Wu, S. H.; Biswas, R.; Riche, C. T.; Povinelli, M. L.; Malmstadt, N. The Dynamics of Giant Unilamellar Vesicle Oxidation Probed by Morphological Transitions. *Biochim. Biophys. Acta - Biomembr.* **2014**, *1838* (10), 2615–2624.

(28) Scholz, S.; Kondakov, D.; Lüssem, B.; Leo, K. Degradation Mechanisms and Reactions in Organic Light-Emitting Devices. *Chem. Rev.* **2015**, *115* (16), 8449–8503.

(29) Pavani, C.; Iamamoto, Y.; Baptista, M. S. Mechanism and Efficiency of Cell Death of Type II Photosensitizers: Effect of Zinc Chelation. *Photochem. Photobiol.* **2012**, *88* (4), 774–781.

(30) Ben Amor, T.; Jori, G. Sunlight-Activated Insecticides: Historical Background and Mechanisms of Phototoxic Activity. *Insect Biochem. Mol. Biol.* **2000**, *30* (10), 915–925.

(31) Anderson, S. M.; Krinsky, N. I. Protective Action of Carotenoid Pigments against Photodynamic Damage to Liposomes. *Photochem. Photobiol.* **1973**, *18* (5), 403–408.

(32) Boonnoy, P.; Jarerattanachat, V.; Karttunen, M.; Wong-ekkabut, J. Bilayer Deformation, Pores, and Micellation Induced by Oxidized Lipids. *J. Phys. Chem. Lett.* **2015**, *6* (24), 4884–4888.

(33) Yusupov, M.; Van der Paal, J.; Neyts, E. C.; Bogaerts, A. Synergistic Effect of Electric Field and Lipid Oxidation on the Permeability of Cell Membranes. *Biochim. Biophys. Acta - Gen. Subj.* **2017**, *1861* (4), 839–847.

(34) Van der Paal, J.; Neyts, E. C.; Verlackt, C. C. W.; Bogaerts, A. Effect of Lipid Peroxidation on Membrane Permeability of Cancer and Normal Cells Subjected to Oxidative Stress. *Chem. Sci.* **2016**, *7* (1), 489–498.

(35) Neto, A. J. P.; Cordeiro, R. M. Molecular Simulations of the Effects of Phospholipid and Cholesterol Peroxidation on Lipid Membrane Properties. *Biochim. Biophys. Acta - Biomembr.* **2016**, *1858* (9), 2191–2198.

(36) Runas, K. A.; Malmstadt, N. Low Levels of Lipid Oxidation Radically Increase the Passive Permeability of Lipid Bilayers. *Soft Matter* **2015**, *11* (3), 499–505.

(37) Runas, K. A.; Acharya, S. J.; Schmidt, J. J.; Malmstadt, N. Addition of Cleaved Tail Fragments during Lipid Oxidation Stabilizes Membrane Permeability Behavior. *Langmuir* **2016**, *32* (3), 779–786.

(38) Ytzhak, S.; Ehrenberg, B. The Effect of Photodynamic Action on Leakage of Ions through Liposomal Membranes That Contain Oxidatively Modified Lipids. *Photochem. Photobiol.* **2014**, *90* (4), 796–800.

(39) Bacellar, I. O. L.; Pavani, C.; Sales, E. M.; Itri, R.; Wainwright, M.; Baptista, M. S. Membrane Damage Efficiency of Phenothiazinium Photosensitizers. *Photochem. Photobiol.* **2014**, *90* (4), 801–813.

(40) Wilkinson, F.; Helman, W. P.; Ross, A. B. Quantum Yields for the Photosensitized Formation of the Lowest Electronically Excited Singlet State of Molecular Oxygen in Solution. *J. Phys. Chem. Ref. Data* **1993**, *22* (1), 113–262.

(41) Wainwright, M.; Giddens, R. M. Phenothiazinium Photosensitisers: Choices in Synthesis and Application. *Dye. Pigment.* **2003**, *57* (3), 245–257.

(42) Noodt, B. B.; Rodal, G. H.; Wainwright, M.; Peng, Q.; Horobin, R.; Nesland, J. M.; Berg, K. Apoptosis Induction by Different Pathways with Methylene Blue Derivative and Light from Mitochondrial Sites in V79 Cells. *Int. J. cancer* **1998**, *75* (6), 941–948.

(43) Tanielian, C.; Mechin, R. Reaction and Quenching of Singlet Molecular Oxygen with Esters of Polyunsaturated Fatty Acids. *Photochem. Photobiol.* **1994**, *59* (3), 263–268.

(44) Huvaere, K.; Cardoso, D. R.; Homem-De-Mello, P.; Westermann, S.; Skibsted, L. H. Light-Induced Oxidation of Unsaturated Lipids as Sensitized by Flavins. *J. Phys. Chem. B* **2010**, *114* (16), 5583–5593.

(45) Chacon, J. N.; McLearie, J.; Sinclair, R. S. Singlet Oxygen Yields and Radical Contributions in the Dye-Sensitised Photo-Oxidation in Methanol of Esters of Polyunsaturated Fatty Acids (Oleic, Linoleic, Linolenic and Arachidonic). *Photochem. Photobiol.* **1988**, *47* (5), 647–656.

(46) Luo, D.; Li, N.; Carter, K. A.; Lin, C.; Geng, J.; Shao, S.; Huang, W.-C.; Qin, Y.; Atilla-Gokcumen, G. E.; Lovell, J. F. Rapid Light-Triggered Drug Release in Liposomes Containing Small Amounts of Unsaturated and Porphyrin-Phospholipids. *Small* **2016**, *12* (22), 3039–3047.

(47) Russell, G. A. Deuterium-Isotope Effects in the Autoxidation of Aralkyl Hydrocarbons. Mechanism of the Interaction of Peroxy Radicals. *J. Am. Chem. Soc.* **1957**, *79* (14), 3871–3877.

(48) Miyamoto, S.; Martinez, G. R.; Medeiros, M. H. G.; Di Mascio, P. Singlet Molecular Oxygen Generated from Lipid Hydroperoxides by the Russell Mechanism: Studies Using 18 O-Labeled Linoleic Acid Hydroperoxide and Monomol Light Emission Measurements. *J. Am. Chem. Soc.* **2003**, *125* (20), 6172–6179.

(49) Mansano, F. V.; Kazaoka, R. M. A.; Ronsein, G. E.; Prado, F. M.; Genaro-Mattos, T. C.; Uemi, M.; Di Mascio, P.; Miyamoto, S. Highly Sensitive Fluorescent Method for the Detection of Cholesterol Aldehydes Formed by Ozone and Singlet Molecular Oxygen. *Anal. Chem.* **2010**, *82* (16), 6775–6781.

(50) Nohta, H.; Sonoda, J.; Yoshida, H.; Satozono, H.; Ishida, J.; Yamaguchi, M. Liquid Chromatographic Determination of Dicarboxylic Acids Based on Intramolecular Excimer-Forming Fluorescence Derivatization. *J. Chromatogr. A* **2003**, *1010* (1), 37–44.

(51) Marrink, S.-J.; Berendsen, H. J. C. Simulation of Water Transport through a Lipid Membrane. *J. Phys. Chem.* **1994**, *98* (15), 4155–4168.

(52) Qiao, B.; Olvera de la Cruz, M. Driving Force for Water Permeation Across Lipid Membranes. *J. Phys. Chem. Lett.* **2013**, *4* (19), 3233–3237.

(53) Paula, S.; Volkov, A. G.; Van Hoek, A. N.; Haines, T. H.; Deamer, D. W. Permeation of Protons, Potassium Ions, and Small Polar Molecules through Phospholipid Bilayers as a Function of Membrane Thickness. *Biophys. J.* **1996**, *70* (1), 339–348.

(54) Sugii, T.; Takagi, S.; Matsumoto, Y. A Molecular-Dynamics Study of Lipid Bilayers: Effects of the Hydrocarbon Chain Length on Permeability. *J. Chem. Phys.* **2005**, *123* (18), 184714.

(55) Gauthier, A.; Joós, B. Stretching Effects on the Permeability of Water Molecules across a Lipid Bilayer. *J. Chem. Phys.* **2007**, *127* (10), 105104.

(56) Shinoda, W. Permeability across Lipid Membranes. *Biochim. Biophys. Acta - Biomembr.* **2016**, *1858* (10), 2254–2265.

(57) Lis, M.; Wizert, A.; Przybylo, M.; Langner, M.; Swiatek, J.; Jungwirth, P.; Cwiklik, L. The Effect of Lipid Oxidation on the Water Permeability of Phospholipids Bilayers. *Phys. Chem. Chem. Phys.* **2011**, *13* (39), 17555.

(58) Ferreira, T. M.; Sood, R.; Bärenwald, R.; Carlström, G.; Topgaard, D.; Saalwächter, K.; Kinnunen, P. K. J.; Ollila, O. H. S. Acyl Chain Disorder and Azelaoyl Orientation in Lipid Membranes Containing Oxidized Lipids. *Langmuir* **2016**, *32* (25), 6524–6533.

(59) Bachowski, G. J.; Ben-Hur, E.; Girotti, A. W. Phthalocyanine-Sensitized Lipid Peroxidation in Cell Membranes: Use of Cholesterol and Azide as Probes of Primary Photochemistry. *J. Photochem. Photobiol. B.* **1991**, *9* (3–4), 307–321.

(60) Woodward, R. B. Structure and the Absorption Spectra of α,β-Unsaturated Ketones. *J. Am. Chem. Soc.* **1941**, *63* (4), 1123–1126.

(61) Yin, H.; Xu, L.; Porter, N. A. Free Radical Lipid Peroxidation: Mechanisms and Analysis. *Chem. Rev.* **2011**, *111* (10), 5944–5972.

(62) Tanielian, C.; Mechin, R.; Shakirullah, M. Origin of Dye Bleaching and Polymer Degradation in the Methylene Blue-Sensitized Photo-Oxygenation of Polybutadiene. *J. Photochem. Photobiol. A Chem.* **1992**, *64* (2), 191–199.

(63) Tanielian, C.; Mechin, R. Alkyl Hydroperoxides as Electron Donors in Photochemical Reactions. *J. Photochem. Photobiol. A Chem.* **1997**, *107* (1–3), 291–293.

(64) Krumova, K.; Friedland, S.; Cosa, G. How Lipid Unsaturation, Peroxyl Radical Partitioning, and Chromanol Lipophilic Tail Affect the Antioxidant Activity of α-Tocopherol: Direct Visualization via High-Throughput Fluorescence Studies Conducted with Fluorogenic α-Tocopherol Analogues. *J. Am. Chem. Soc.* **2012**, *134* (24), 10102–10113.

(65) Anbar, M.; Loewenstein, A.; Meiboom, S. Kinetics of Hydrogen Exchange between Hydrogen Peroxide and Water Studied by Proton Magnetic Resonance. *J. Am. Chem. Soc.* **1958**, *80* (11), 2630–2634.

(66) Burton, G. W.; Ingold, K. U. Autoxidation of Biological Molecules. 1. Antioxidant Activity of Vitamin E and Related Chain-Breaking Phenolic Antioxidants in Vitro. *J. Am. Chem. Soc.* **1981**, *103* (21), 6472–6477.

(67) Witting, P. K.; Bowry, V. W.; Stocker, R. Inverse Deuterium Kinetic Isotope Effect for Peroxidation in Human Low-Density Lipoprotein (LDL): A Simple Test for Tocopherol-Mediated Peroxidation of LDL Lipids. *FEBS Lett.* **1995**, *375* (1–2), 45–49.

(68) Bowry, V. W.; Ingold, K. U. The Unexpected Role of Vitamin E (α-Tocopherol) in the Peroxidation of Human Low-Density Lipoprotein 1. *Acc. Chem. Res.* **1999**, *32* (1), 27–34.

(69) Oleynik, P.; Ishihara, Y.; Cosa, G. Design and Synthesis of a BODIPY-α-Tocopherol Adduct for Use as an Off/On Fluorescent Antioxidant Indicator. *J. Am. Chem. Soc.* **2007**, *129* (7), 1842–1843.

(70) Gardner, H. W. Oxygen Radical Chemistry of Polyunsaturated Fatty Acids. *Free Radic. Biol. Med.* **1989**, *7* (1), 65–86.

(71) Hock Rearrangement. In *Comprehensive Organic Name Reactions and Reagents*; John Wiley & Sons, Inc.: Hoboken, NJ, USA, 2010.

(72) Schneider, C.; Porter, N. A.; Brash, A. R. Routes to 4-Hydroxynonenal: Fundamental Issues in the Mechanisms of Lipid Peroxidation. *J. Biol. Chem.* **2008**, *283* (23), 15539–15543.

(73) Morita, M.; Tokita, M. Hydroxy Radical, Hexanal, and Decadienal Generation by Autocatalysts in Autoxidation of Linoleate Alone and with Eleostearate. *Lipids* **2008**, *43* (7), 589–597.

(74) Paul, H.; Small, R. D.; Scaiano, J. C. Hydrogen Abstraction by Tert-Butoxy Radicals. A Laser Photolysis and Electron Spin Resonance Study. *J. Am. Chem. Soc.* **1978**, *100* (14), 4520–4527.

(75) Foote, C. S. Mechanisms of Photosensitized Oxidation. *Science* **1968**, *162* (3857), 963–970.

(76) Albani, B. A.; Peña, B.; Leed, N. A.; de Paula, N. A. B. G.; Pavani, C.; Baptista, M. S.; Dunbar, K. R.; Turro, C. Marked Improvement in Photoinduced Cell Death by a New Tris-Heteroleptic Complex with Dual Action: Singlet Oxygen Sensitization and Ligand Dissociation. *J. Am. Chem. Soc.* **2014**, *136* (49), 17095–17101.

(77) Petroselli, G.; Dántola, M. L.; Cabrerizo, F. M.; Capparelli, A. L.; Lorente, C.; Oliveros, E.; Thomas, A. H. Oxidation of 2′-Deoxyguanosine 5′-Monophosphate Photoinduced by Pterin: Type I versus Type II Mechanism. *J. Am. Chem. Soc.* **2008**, *130* (10), 3001–3011.

(78) Cardoso, D. R.; Olsen, K.; Skibsted, L. H. Mechanism of Deactivation of Triplet-Excited Riboflavin by Ascorbate, Carotenoids, and Tocopherols in Homogeneous and Heterogeneous Aqueous Food Model Systems. *J. Agric. Food Chem.* **2007**, *55* (15), 6285–6291.

(79) Stockwell, B. R.; Friedmann Angeli, J. P.; Bayir, H.; Bush, A. I.; Conrad, M.; Dixon, S. J.; Fulda, S.; Gascón, S.; Hatzios, S. K.; Kagan, V. E.; Noel, K.; Jiang, X.; Linkermann, A.; Murphy, M. E.; Overholtzer, M.; Oyagi, A.; Pagnussat, G. C.; Park, J.; Ran, Q.; Rosenfeld, C. S.; Salnikow, K.; Tang, D.; Torti, F. M.; Torti, S. V.; Toyokuni, S.; Woerpel, K. A.; Zhang, D. D. Ferroptosis: A Regulated Cell Death Nexus Linking Metabolism, Redox Biology, and Disease. *Cell* **2017**, *171* (2), 273–285.

For Table of Contents Only

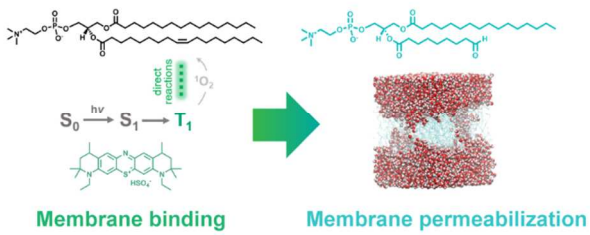

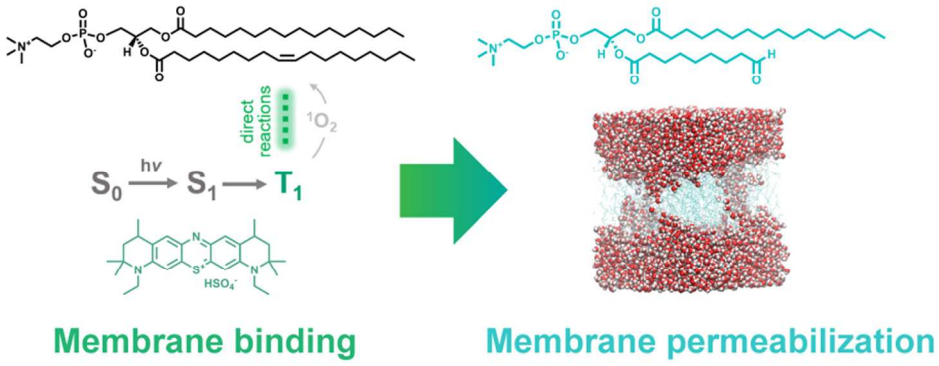

82x32mm (300 x 300 DPI)

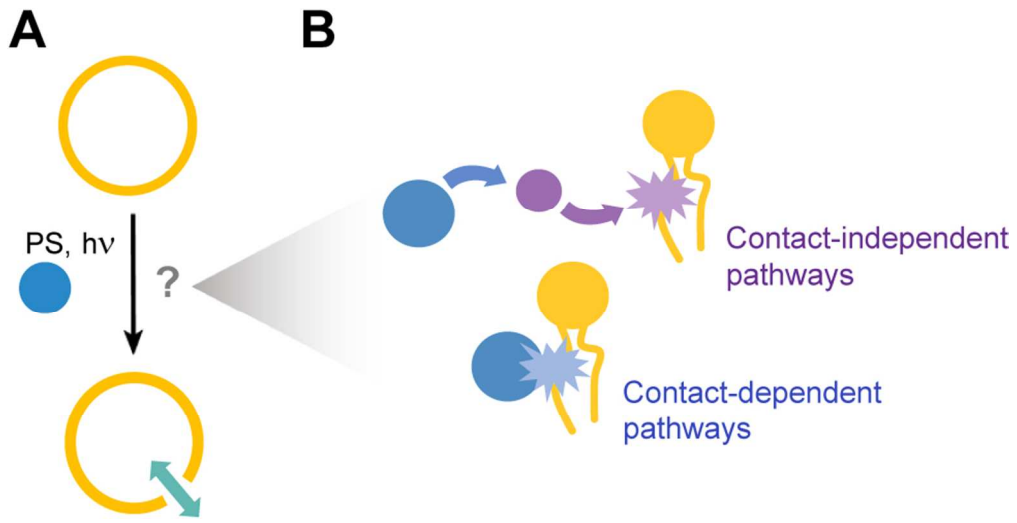

82x42mm (300 x 300 DPI)

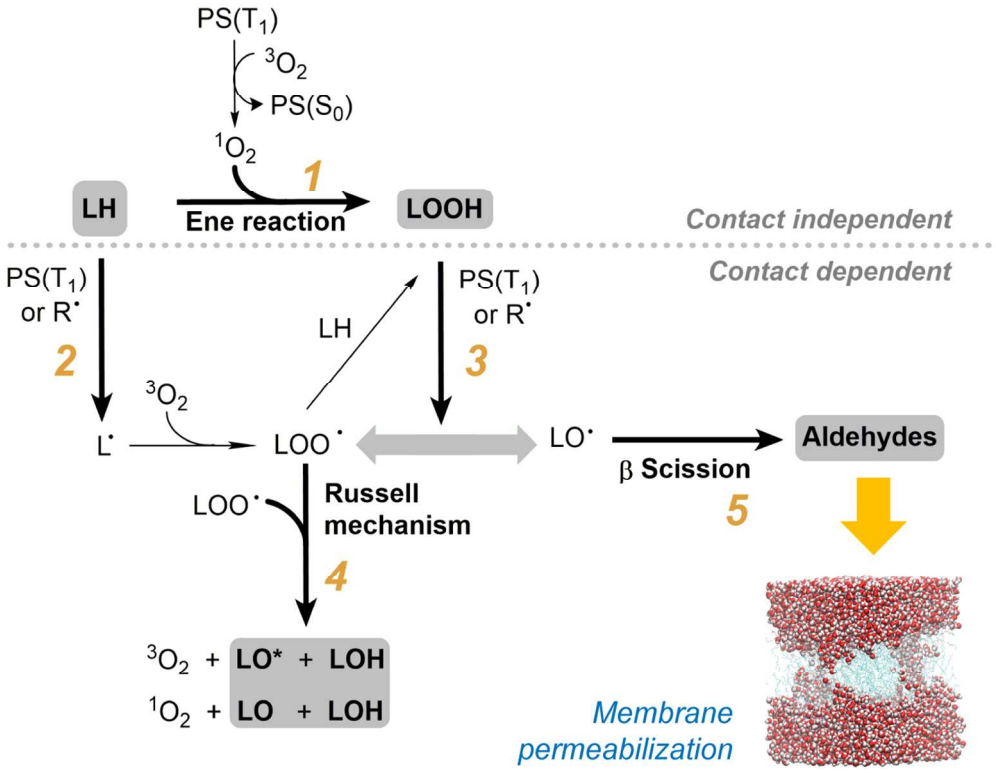

120x92mm (300 x 300 DPI)

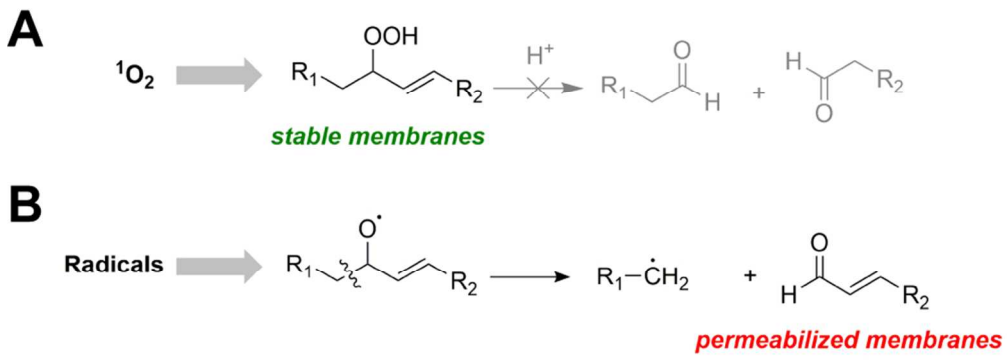

84x30mm (300 x 300 DPI)

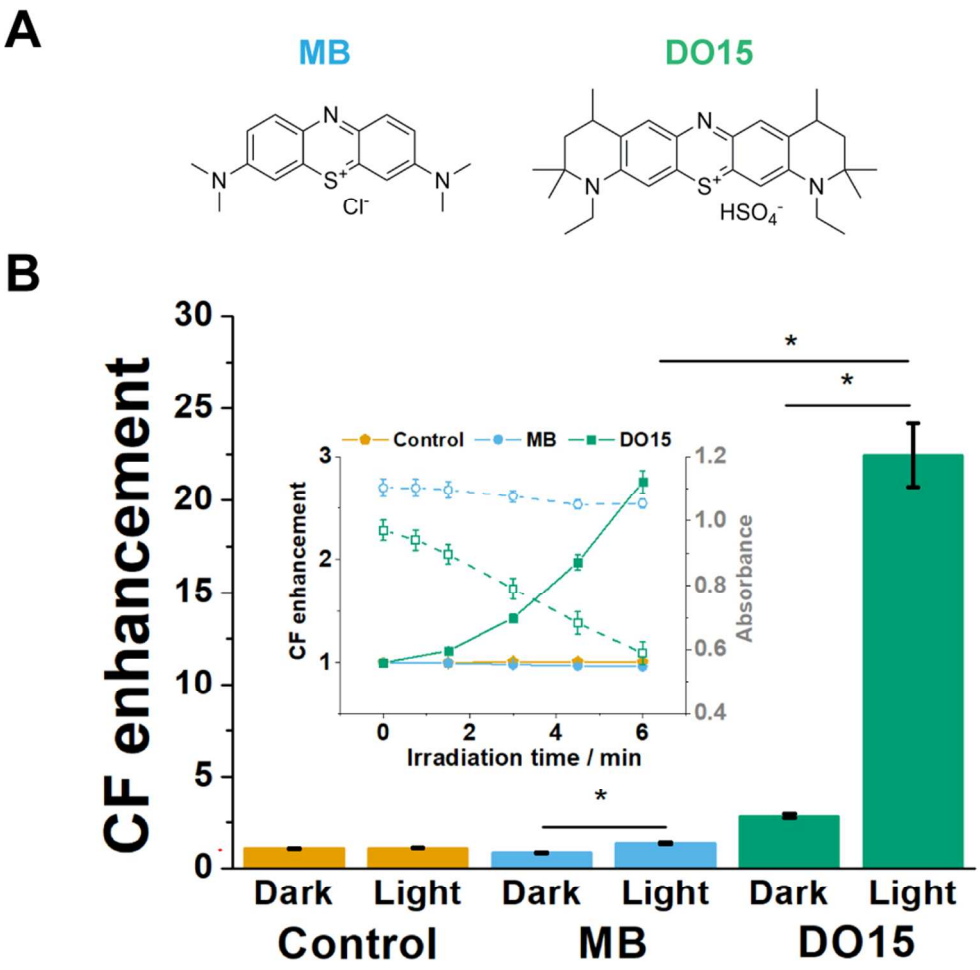

82x81mm (300 x 300 DPI)

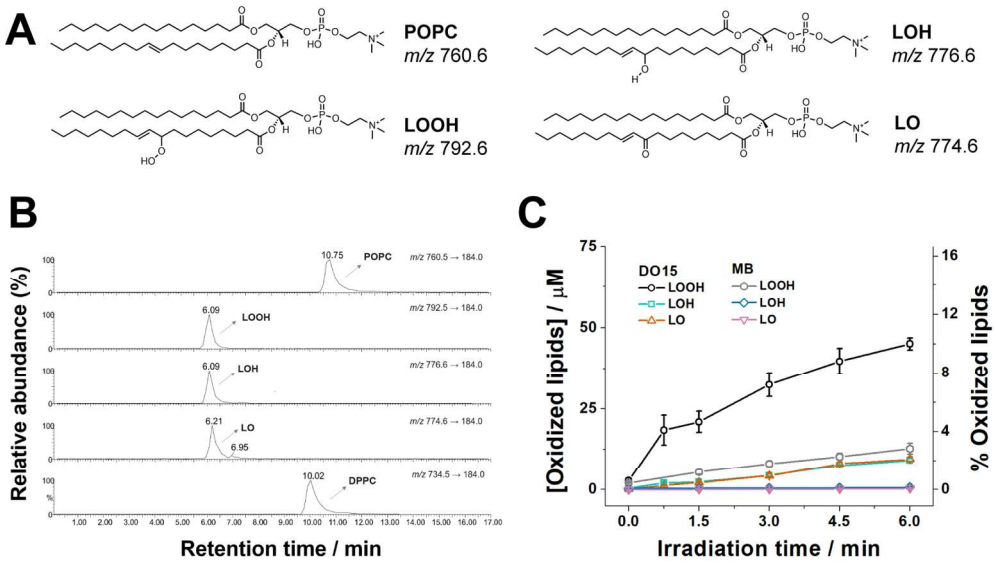

147x83mm (300 x 300 DPI)

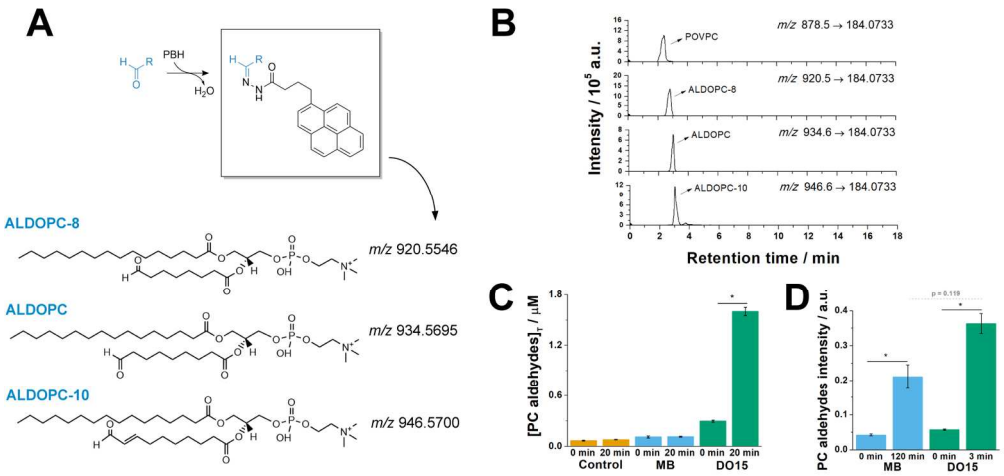

168x80mm (300 x 300 DPI)

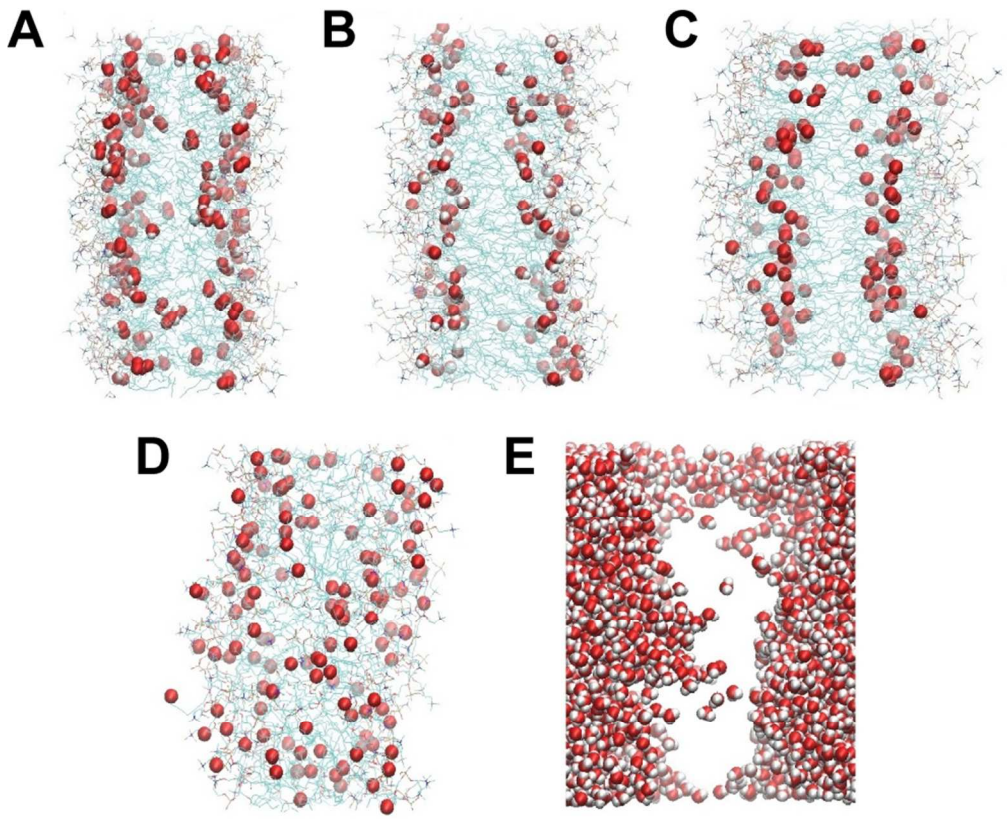

83x68mm (300 x 300 DPI)

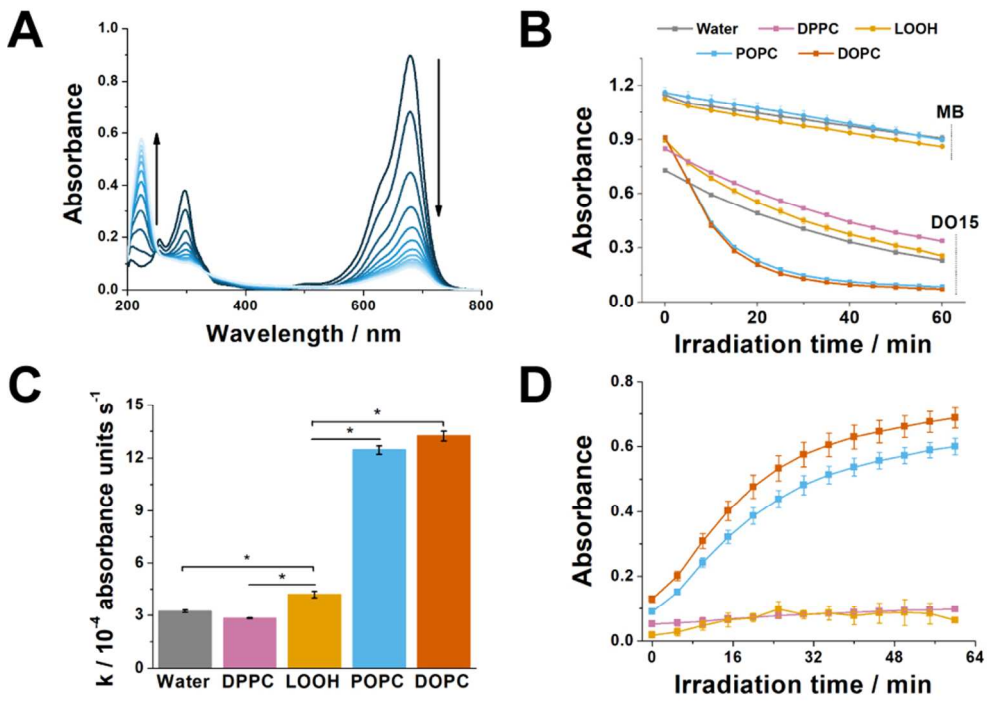

84x59mm (300 x 300 DPI)

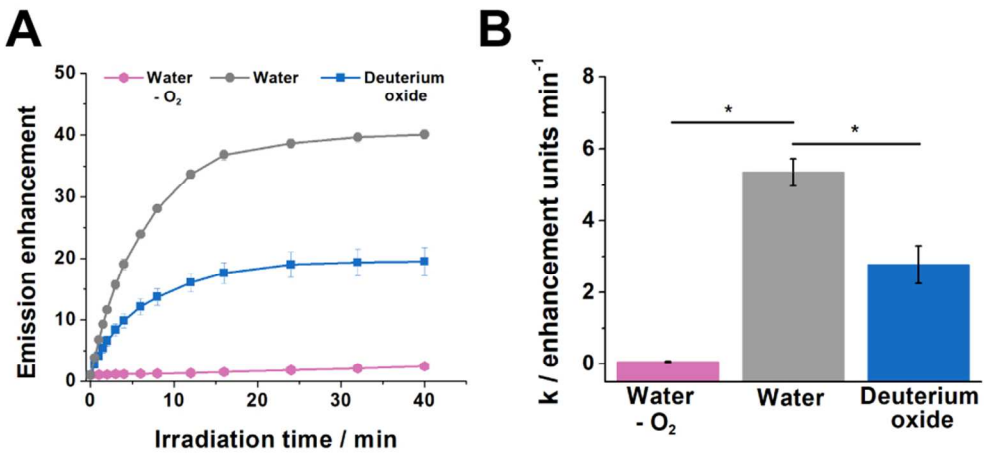

83x37mm (300 x 300 DPI)